Cell

Transcriptional Amplification in Tumor Cells with Elevated c-Myc

Charles Y. Lin,[1,2,6] Jakob Lovén,[1,6] Peter B. Rahl,[1,6] Ronald M. Paranal,[3] Christopher B. Burge,[4] James E. Bradner,[3,5] Tong Ihn Lee,[1] and Richard A. Young[1,4,*]

[1]Whitehead Institute for Biomedical Research, 9 Cambridge Center, Cambridge, MA 02142, USA
[2]Computational and Systems Biology Program
[4]Department of Biology
Massachusetts Institute of Technology, Cambridge, MA 02139, USA
[3]Department of Medical Oncology, Dana-Farber Cancer Institute, 450 Brookline Avenue, Boston, MA 02215, USA
[5]Department of Medicine, Harvard Medical School, 25 Shattuck Street, Boston, MA 02115, USA
[6]These authors contributed equally
*Correspondence: young@wi.mit.edu
http://dx.doi.org/10.1016/j.cell.2012.08.026

SUMMARY

Elevated expression of the c-Myc transcription factor occurs frequently in human cancers and is associated with tumor aggression and poor clinical outcome. The effect of high levels of c-Myc on global gene regulation is poorly understood but is widely thought to involve newly activated or repressed "Myc target genes." We report here that in tumor cells expressing high levels of c-Myc the transcription factor accumulates in the promoter regions of active genes and causes transcriptional amplification, producing increased levels of transcripts within the cell's gene expression program. Thus, rather than binding and regulating a new set of genes, c-Myc amplifies the output of the existing gene expression program. These results provide an explanation for the diverse effects of oncogenic c-Myc on gene expression in different tumor cells and suggest that transcriptional amplification reduces rate-limiting constraints for tumor cell growth and proliferation.

INTRODUCTION

MYC is a potent oncogene that can promote tumorigenesis in a wide range of tissues (Felsher and Bishop, 1999; Flores et al., 2004; Jain et al., 2002; Pelengaris et al., 1999; Sodir et al., 2011; Soucek et al., 2008; Verbeek et al., 1991). *MYC* is the most frequently amplified oncogene and the elevated expression of its gene product, the transcription factor c-Myc, correlates with tumor aggression and poor clinical outcome (Beroukhim et al., 2010; Nesbit et al., 1999). Elevated expression of c-Myc occurs through multiple mechanisms in tumor cells, including gene amplification, chromosomal translocation, single nucleotide polymorphism in regulatory regions, mutation of upstream signaling pathways, and mutations that enhance the stability of the protein (Eilers and Eisenman, 2008; Meyer and Penn, 2008; Pomerantz et al., 2009; Wright et al., 2010). Despite considerable study, it is not yet clear how elevated levels of c-Myc reprograms cells to promote the cancer state.

In normal cells, c-Myc links growth factor stimulation and cellular proliferation (Dang, 2012; Eilers and Eisenman, 2008; Meyer and Penn, 2008). Mitogenic growth factor signaling induces *MYC* expression, and c-Myc is thought to enhance transcription of proliferation-associated genes (Dang, 2012; Eilers and Eisenman, 2008; Meyer and Penn, 2008). In tumor cells that express high levels of c-Myc, cellular proliferation is no longer dependent on growth-factor stimulation, and this uncoupling from growth factor regulation leads to the uncontrolled proliferation characteristic of cancer cells. Elevated expression of c-Myc also causes changes in chromatin structure, ribosome biogenesis, metabolic pathways, cell adhesion, cell size, apoptosis, and angiogenesis, among others (Amati et al., 1998; Amati et al., 2001; Cole and Cowling, 2008; Cowling and Cole, 2010; Dai and Lu, 2008; Dang, 2010; Eilers and Eisenman, 2008; Facchini and Penn, 1998; Gallant, 2005; Hanahan and Weinberg, 2011; Herold et al., 2009; Hoffman and Liebermann, 2008; Hurlin and Dezfouli, 2004; Kuttler and Mai, 2006; Lin et al., 2009; Meyer and Penn, 2008; Nieminen et al., 2007; Nilsson and Cleveland, 2003; Peterson and Ayer, 2011; Prochownik, 2008; Ruggero, 2009; Secombe et al., 2004; Shchors and Evan, 2007; Singh and Dalton, 2009; van Riggelen et al., 2010). How elevated levels of c-Myc cause such a broad spectrum of cellular effects is not understood.

c-Myc's identity as a DNA-binding transcription factor suggests that the set of genes that are bound and regulated by the factor are key to explaining much of c-Myc's role in cancer. c-Myc is a basic helix loop helix (bHLH) transcription factor that forms a heterodimer with Max and binds to E-box sequences near the core promoter elements of actively transcribed genes (Blackwood and Eisenman, 1991). Numerous studies have identified c-Myc target genes in a variety of tumor cells (Dang et al., 2006; Ji et al., 2011; Kim et al., 2006; Schlosser et al., 2005; Schuhmacher et al., 2001; Zeller et al., 2003). Interestingly, these "c-Myc target signatures" show little overlap (Chandriani et al., 2009), which has made it difficult to ascribe c-Myc's oncogenic properties to any one set of target genes. The relatively small set of genes that are common to c-Myc target signatures are

generally involved in core proliferation and metabolism processes (Ji et al., 2011) but do not account for the wide variety of cellular effects ascribed to oncogenic c-Myc.

Some studies suggest that c-Myc may play a different role than conventional transcription factors. Although many transcription factors activate gene expression by recruiting the transcription apparatus to promoters, studies in embryonic stem cells argue that c-Myc binds the core promoter region of a large fraction of actively transcribed genes and functions to enhance transcription elongation (Rahl et al., 2010). In tumor cells, there is evidence that c-Myc can function to stimulate transcription elongation at certain genes (Bouchard et al., 2004; Brès et al., 2009; Eberhardy and Farnham, 2001, 2002; Gargano et al., 2007; Kanazawa et al., 2003). These findings led us to consider the possibility that in tumor cells expressing high levels of c-Myc, the factor binds most actively transcribed genes and causes increased expression of all of these genes, as opposed to the prevailing model that it regulates a specific cohort of target genes.

We describe here how c-Myc occupies and regulates genes throughout the genome in tumor cells that express various levels of this oncoprotein. In tumor cells expressing low levels of c-Myc, the transcription factor is bound almost exclusively to E-box sequences in the core promoter elements of most actively transcribed genes. In tumor cells with elevated levels of c-Myc, we find the transcription factor at the same set of active genes, but now at elevated levels, occupying both the core promoters and the enhancers of these active genes at additional, low-affinity E-box-like sequences. The increase in c-Myc occupancy leads to increased transcription elongation by RNA polymerase II (RNA Pol II) and increased levels of transcripts per cell. We conclude that high levels of c-Myc in tumor cells causes transcriptional amplification, producing elevated levels of transcripts from the existing gene expression program of tumor cells.

RESULTS

Increased c-Myc Leads to Increased Binding to Promoters of Active Genes

To investigate the effects of increased levels of c-Myc on its genome wide occupancy and on gene expression, we used the human P493-6 B cell model of Burkitt's lymphoma (Pajic et al., 2000; Schuhmacher et al., 1999). In these cells, which contain a tetracycline (Tet)-repressible *MYC* transgene, *MYC* expression can be reduced to very low levels and then reactivated such that the levels of c-Myc protein gradually increase (Figures 1A and 1B). The P493-6 cells contained 13,000, 76,500, and 362,000 molecules of c-Myc/cell at 0, 1, and 24 hr, respectively, after induction (Figure 1C), and the majority of this protein accumulated in the nucleus (Figure 1D; Figure S1A available online).

To investigate the relationship between c-Myc levels and c-Myc genome occupancy in P493-6 cells, we used chromatin immunoprecipitation coupled to high-throughput sequencing (ChIP-Seq) with antibodies specific for c-Myc at 0, 1, and 24 hr after *MYC* induction. Previous studies have shown that c-Myc tends to occupy the promoter regions of protein-coding genes (Chen et al., 2008; Fernandez et al., 2003; Guccione et al., 2006; Kidder et al., 2008; Li et al., 2003; Rahl et al., 2010; Zeller et al., 2006), so we focused our initial analysis on the 2 kb regions surrounding the transcription start sites of such genes. The results showed that c-Myc generally occupies the core promoters of actively transcribed genes, as evidenced by co-occupancy with RNA Pol II (Figure 1E). Furthermore, increased levels of c-Myc led to increased c-Myc signal at the core promoters of these genes, as evidenced by inspection of individual gene tracks and genome-wide analysis (Figures 1E–1H). Interestingly, the effect of increasing c-Myc levels by 28-fold in this system had only a small effect on the total number of genes that were bound by c-Myc or the total number that were actively transcribed (Figure 1I, Table S1). Instead, the predominant effect of increased levels of c-Myc was increased binding to the promoters of the same set of active genes.

The DNA binding and transcriptional activities of c-Myc require heterodimerization with Max (Blackwood and Eisenman, 1991; Blackwood et al., 1992; Prendergast et al., 1991), so all sites bound by c-Myc should be bound by Max. Indeed, ChIP-seq analysis revealed that Max co-occupied essentially all c-Myc-bound promoter sites (Figure S1B). Furthermore, analysis of the c-Myc binding sites at core promoters revealed these sequences are highly enriched for the known c-Myc/Max E-box binding motif (CACGTG) (p value $< 1 \times 10^{-232}$). These results indicate that increased expression of c-Myc in P493-6 cells leads to increased binding by c-Myc/Max heterodimers at the E-box-containing core promoter sequences of actively transcribed genes.

Increased c-Myc Leads to Enhancer Binding

A search for c-Myc binding events outside the core promoter regions of protein-coding genes revealed that enhancers associated with active genes became occupied by c-Myc in cells with elevated levels of the factor (Figure 2). It was also evident that rRNA and tRNA genes became occupied by c-Myc (Figure 2A), as reported previously (Arabi et al., 2005; Gomez-Roman et al., 2003; Grandori et al., 2005). c-Myc was not enriched at transcriptionally silent genes (genes lacking evidence of RNA Pol II) in cells with low or high levels of the factor.

Increases in the levels of c-Myc led to substantial increases in its levels at enhancers of active genes (Figures 2B and 2C; Figures S2A and S2B). As expected, the c-Myc heterodimer partner, Max, occupied essentially all the enhancer sites that were bound by c-Myc (Figure S2C). Analysis of the sequences at enhancer elements revealed that an E-box variant motif is highly enriched at these sites (p value $< 4 \times 10^{-775}$) (Figure 2D). These results are consistent with the expectation that c-Myc occupies the E-box variant sequences at enhancers as a c-Myc/Max heterodimer.

In cells expressing high levels of c-Myc, the number of molecules of the factor (362,000) exceeds the number of active core promoters (16,500). We reasoned that E-box sequences in core promoter regions would therefore become saturated as the levels of c-Myc increased, and the factor would then bind lower affinity E-box sequences that occur at core promoters and enhancers. To test this idea, we ranked all E-box (CANNTG) variants present in core promoter and enhancer regions by c-Myc binding signal in the 24 hr ChIP-Seq data, and determined

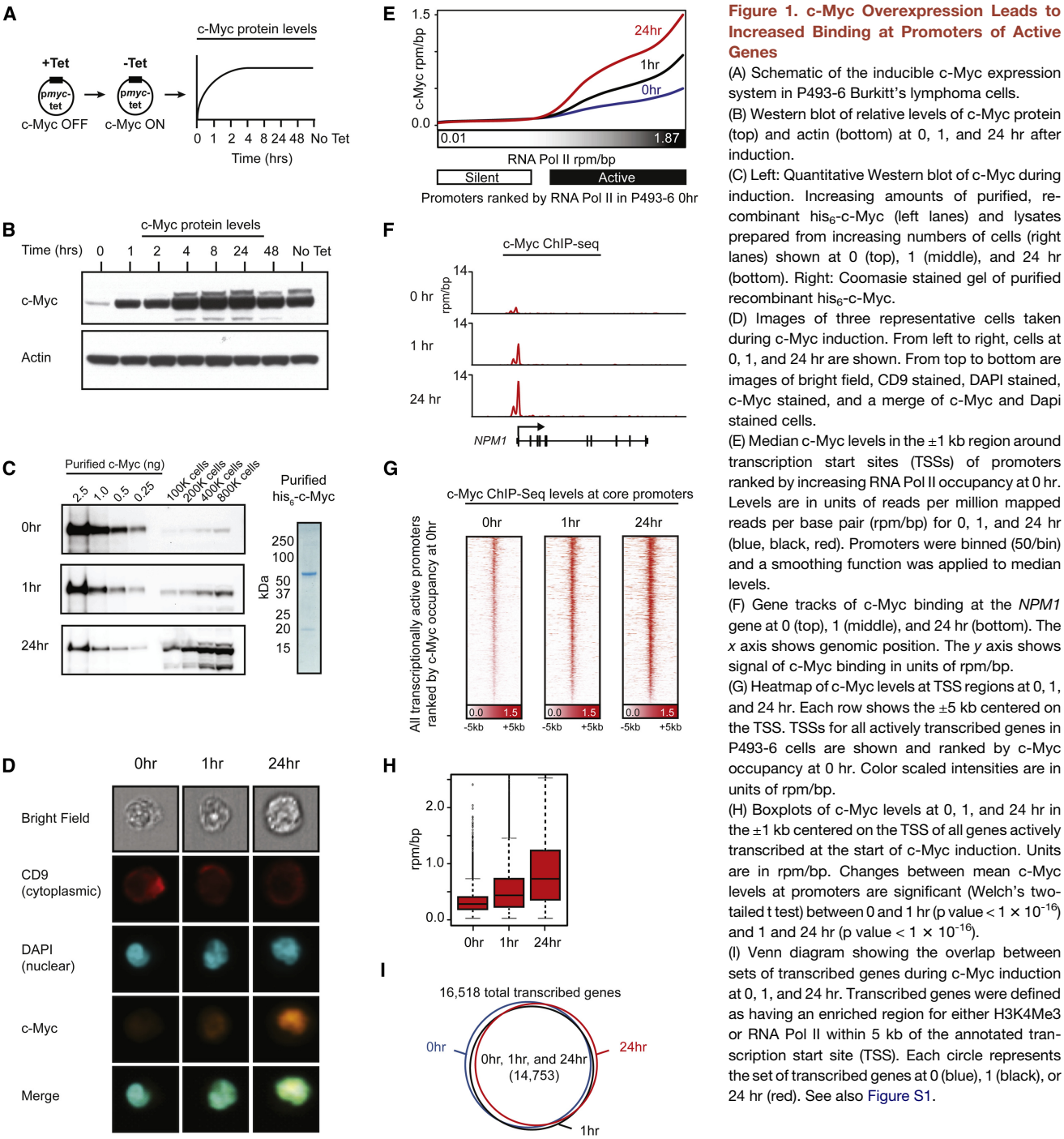

Figure 1. c-Myc Overexpression Leads to Increased Binding at Promoters of Active Genes

(A) Schematic of the inducible c-Myc expression system in P493-6 Burkitt's lymphoma cells.

(B) Western blot of relative levels of c-Myc protein (top) and actin (bottom) at 0, 1, and 24 hr after induction.

(C) Left: Quantitative Western blot of c-Myc during induction. Increasing amounts of purified, recombinant his_6-c-Myc (left lanes) and lysates prepared from increasing numbers of cells (right lanes) shown at 0 (top), 1 (middle), and 24 hr (bottom). Right: Coomasie stained gel of purified recombinant his_6-c-Myc.

(D) Images of three representative cells taken during c-Myc induction. From left to right, cells at 0, 1, and 24 hr are shown. From top to bottom are images of bright field, CD9 stained, DAPI stained, c-Myc stained, and a merge of c-Myc and Dapi stained cells.

(E) Median c-Myc levels in the ±1 kb region around transcription start sites (TSSs) of promoters ranked by increasing RNA Pol II occupancy at 0 hr. Levels are in units of reads per million mapped reads per base pair (rpm/bp) for 0, 1, and 24 hr (blue, black, red). Promoters were binned (50/bin) and a smoothing function was applied to median levels.

(F) Gene tracks of c-Myc binding at the *NPM1* gene at 0 (top), 1 (middle), and 24 hr (bottom). The *x* axis shows genomic position. The *y* axis shows signal of c-Myc binding in units of rpm/bp.

(G) Heatmap of c-Myc levels at TSS regions at 0, 1, and 24 hr. Each row shows the ±5 kb centered on the TSS. TSSs for all actively transcribed genes in P493-6 cells are shown and ranked by c-Myc occupancy at 0 hr. Color scaled intensities are in units of rpm/bp.

(H) Boxplots of c-Myc levels at 0, 1, and 24 hr in the ±1 kb centered on the TSS of all genes actively transcribed at the start of c-Myc induction. Units are in rpm/bp. Changes between mean c-Myc levels at promoters are significant (Welch's two-tailed t test) between 0 and 1 hr (p value $< 1 \times 10^{-16}$) and 1 and 24 hr (p value $< 1 \times 10^{-16}$).

(I) Venn diagram showing the overlap between sets of transcribed genes during c-Myc induction at 0, 1, and 24 hr. Transcribed genes were defined as having an enriched region for either H3K4Me3 or RNA Pol II within 5 kb of the annotated transcription start site (TSS). Each circle represents the set of transcribed genes at 0 (blue), 1 (black), or 24 hr (red). See also Figure S1.

how frequently these various sequences were present in these bound regions (Figure 2E). We found that the highest signals were associated with the canonical CACGTG E-box sequence and that the canonical E-box sequence occurs with the highest frequency (~40%) of all E-box sequences in core promoter regions (Figure 2E). In contrast, the canonical E-box sequence occurs much less frequently in enhancer regions (~15%), where a variety of E-box variants are occupied by c-Myc. To investigate whether there is a relationship between the c-Myc signal at various E-box sequences in the ChIP-Seq data and c-Myc binding affinity for such sequences, we produced recombinant c-Myc/Max protein and studied its binding to DNA fragments containing E-box sequences in vitro by using a gel shift assay (Figure 2F, Figure S2D). The relative affinity of binding to canonical and variant E-box sequences was investigated by incubating c-Myc/Max protein with a DNA fragment containing the

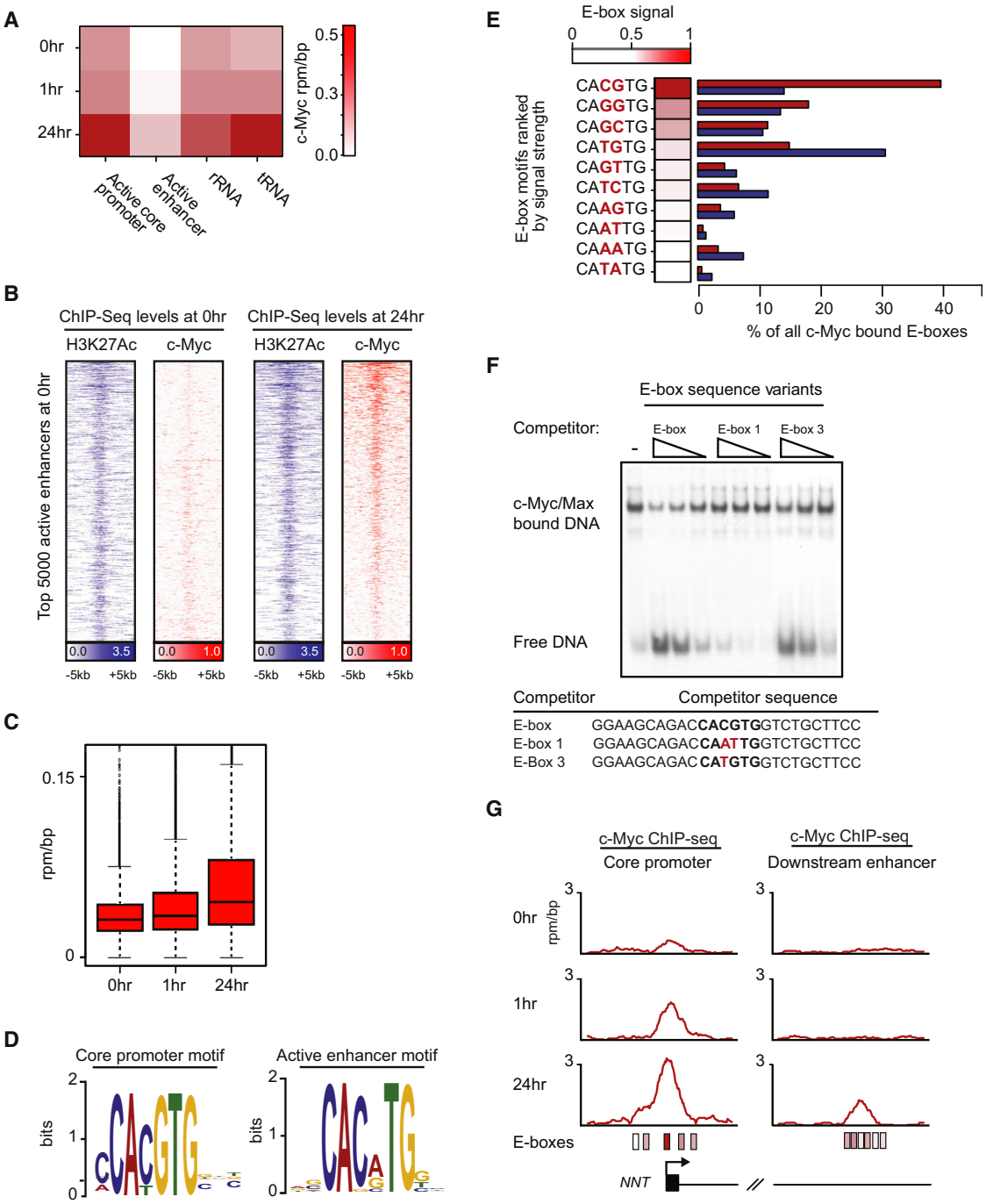

Figure 2. c-Myc Overexpression Leads to Binding of Active Enhancers

(A) Heatmap showing c-Myc occupancy levels at the top 5,000 promoters ranked by RNA Pol II levels at 0 hr, the top 5,000 active enhancers ranked by H3K27Ac levels at 0 hr, rRNA genes, and tRNA genes (columns) at 0, 1, and 24 hr (rows). Intensities are in units of c-Myc rpm/bp.

(B) Heatmap of H3K27Ac and c-Myc levels at the top 5,000 active enhancers ranked by H3K27Ac levels at 0 hr in P493-6 cells at 0 and 24 hr. Each row shows ±5 kb centered on the H3K27Ac peak. Rows are ordered by the net increase in c-Myc occupancy after 24 hr of c-Myc induction. Color scaled intensities are in units of rpm/bp.

(C) Boxplots of c-Myc levels at 0, 1, and 24 hr in the ±1 kb around the center of the top 5,000 active enhancers ranked by H3K27Ac levels at the start of c-Myc induction. Units are in rpm/bp. Changes between mean c-Myc levels at enhancers are significant (Welch's two-tailed t test) between 0 and 1 hr (p value $< 1 \times 10^{-16}$) and 1 and 24 hr (p value $< 1 \times 10^{-16}$).

(D) c-Myc binding motif found enriched at core promoters (left, p value $< 1 \times 10^{-232}$) or at active enhancers (right, p value $< 4 \times 10^{-775}$) 24 hr after c-Myc induction.

canonical E-box in competition with three different DNA fragments. The canonical E-box sequence was the most effective in the competition assay, the E-Box 3 variant CATGTG was less effective, and the E-Box 1 variant CAATTG was least effective (Figure 2F). Thus, for these three E-box sequences, the relative binding signals obtained by ChIP-Seq reflect the relative affinities in this in vitro binding assay. These results are consistent with the model that c-Myc/Max occupies high affinity E-box sequences at core promoters when the protein is present at low levels but then occupies lower affinity E-box sequences at core promoters and enhancers when present at high levels (Figure 2G).

High c-Myc Expression Causes Transcriptional Amplification in Tumor Cells

Previous studies have shown that c-Myc binding can recruit Positive Transcription Elongation Factor b (P-TEFb) and thereby enhance elongation by RNA Pol II at the *CAD* and *CCND2* genes in tumor cells (Bouchard et al., 2004; Eberhardy and Farnham, 2001) and at a large fraction of active genes in embryonic stem cells (Rahl et al., 2010). We therefore investigated whether the elevated levels of c-Myc have these effects at active genes in P493-6 tumor cells.

We first investigated whether increased c-Myc occupancy leads to increased recruitment of the P-TEFb elongation complex genome-wide. At core promoters and enhancers that experienced increased c-Myc occupancy, we detected a significant increase in occupancy by Cdk9, the catalytic subunit of P-TEFb (Figure 3A). For comparison, the levels of the transcription initiation-associated histone H3K4me3 modification showed little or no change at these genes.

We then investigated whether increased c-Myc occupancy results in stimulation of RNA Pol II elongation through increased P-TEFb activity. P-TEFb predominantly phosphorylates the second serine residue of the RNA Pol II C-terminal domain heptad repeat (Zhou et al., 2012). The levels of this elongation-associated Ser2-phosphorylated RNA Pol II (Ser2) and the initiation-associated Ser5-phosphorylated RNA Pol II (Ser5) were measured in P493-6 cells expressing increasing levels of c-Myc (Figure 3B). The levels of the Ser2 RNA Pol II increased 2-fold over the 24 hr time course, whereas the levels of Ser5 RNA Pol II remained largely unchanged, indicating an increase in actively elongating enzyme in cells with increased levels of c-Myc. In addition, we found that increased c-Myc occupancy results in a general and significant increase in the proportion of elongating to initiating RNA Pol II across the genome as measured by ChIP-Seq enrichment (Figure 3C) and traveling ratio (p value $< 1 \times 10^{-5}$) (Figure 3D). As expected, genes with increased c-Myc occupancy at enhancers displayed the greatest increases in elongating RNA Pol II levels (Figure S3A). These results indicate that increased c-Myc binding at active genes stimulates RNA Pol II elongation.

Finally, we determined whether increased c-Myc occupancy results in increases in the absolute levels of RNA. We found that there was a 1.5-fold increase in total RNA levels in cells over the time course of c-Myc induction (Figure 3E). Both rRNA and tRNA levels were increased (Figure 3E; Figure S3B). Digital gene expression (NanoString) (Geiss et al., 2008) was used to quantify mRNA levels/cell for a large set of 1,388 genes selected from multiple functional categories. The results showed that transcripts from 96% of genes that were expressed at reliable levels (one transcript/cell or higher) in cells with relatively low levels of c-Myc were upregulated upon c-Myc induction, with an average 2.4-fold increase in expression (Figure 3F). In contrast, genes that were not expressed in cells with lower levels of c-Myc remained silent (Figure 3F). These results are remarkably consistent with the result, described above, that increasing the levels of c-Myc results in increased binding to the set of existing active genes, with negligible binding to new sets of genes. Together, these results indicate the predominant effect of substantially elevated levels of c-Myc is amplified transcription of the existing gene expression program.

c-Myc Genome Occupancy in Diverse Tumor Cells with Elevated c-Myc

The c-Myc inducible Burkitt's lymphoma model revealed that elevated levels of c-Myc result in increased binding to core promoters and enhancers of active genes, leading to transcriptional amplification. To determine whether high levels of c-Myc leads to similar binding behavior in diverse patient-derived tumor cells, we studied cell lines derived from three different clinically relevant tumor types: small cell lung carcinoma (SCLC), multiple myeloma (MM), and glioblastoma multiforme (GBM). The cell lines used were H2171 (SCLC) (Johnson et al., 1987), which has a c-Myc gene amplification, MM1.S (MM) (Shou et al., 2000), which has an *IGH-MYC* translocation, and U-87 MG (GBM) (Hirvonen et al., 1994), in which c-Myc levels accumulate due to enhanced expression. The levels of c-Myc in these cells were 880,000 molecules/cell in H2171 (SCLC), 495,000 molecules/cell in MM1.S (MM), and 110,000 molecules/cell in U-87 MG (GBM) (Figure 4A), which are similar to the levels observed in the c-Myc inducible Burkitt's lymphoma model between 1

(E) c-Myc occupancy at E-box sequences. Left: E-box variants (CANNTG) were ranked by c-Myc ChIP-Seq signal strength at 24 hr. The signal strength relative to the canonical CACGTG E-box is indicated by the shaded color intensity adjacent to E-box sequences. Right: The percentage of all E-box motifs found in c-Myc bound regions at promoters (red) or enhancers (blue) for all E-box variants.

(F) Gel shift assays of purified c-Myc/Max binding to canonical CACGTG E-box sequences following competition with decreasing amounts (5-, 2.5-, and 1-fold excess) of unlabeled competitor sequences. The higher bands reflect the amounts of labeled canonical E-box sequences bound by c-Myc/Max and the lower band reflects the amount of unbound canonical E-box DNA. Lane 1: No competitor DNA. Lanes 2–10: The effect of adding various amounts of competitor DNA fragments containing the canonical E-box or variant E-box sequence motifs (E-box 1 and E-box 3). Bottom: Competitor DNA sequences are shown centered around the E-box (bold). Differences from the canonical sequence are highlighted in red.

(G) Gene tracks showing c-Myc occupancy (rpm/bp) at the *NNT* promoter (left) or downstream enhancer (right) after 0 (top), 1 (middle), and 24 hr (bottom) after c-Myc induction. The *x* axis shows genomic position. The *y* axis shows signal strength of c-Myc binding. E-boxes proximal to the c-Myc peak at either the promoter or enhancer are depicted as boxes shaded by E-box signal strength (from Figure 2E). The *NNT* gene is indicated at the bottom (introns as lines, exons as boxes). See also Figure S2.

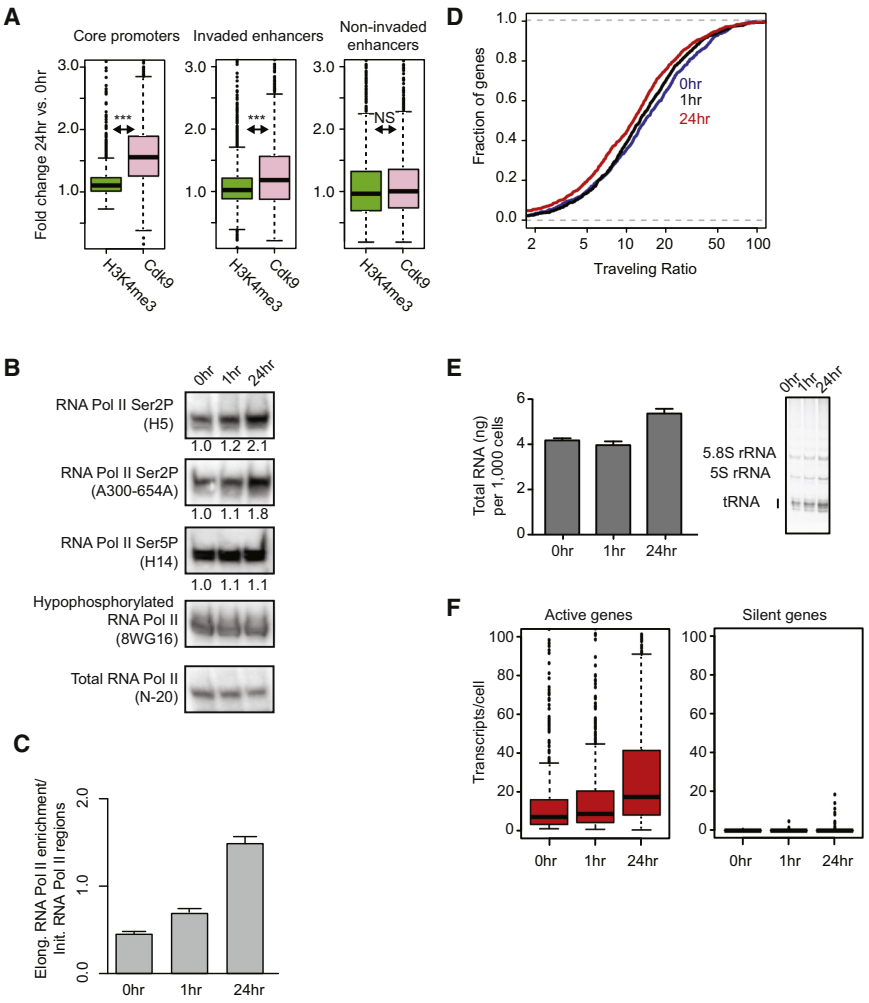

Figure 3. c-Myc Overexpression Leads to Transcriptional Amplification

(A) Boxplots of the fold changes in levels of H3K4Me3 (green) and Cdk9 (pink) between 24 hr and 0 hr at the top 2,000 core promoters with the highest increased c-My occupancy during c-Myc induction (left), the top 2,000 enhancers with the highest increased c-Myc occupancy during c-Myc induction (center), and 2,000 enhancers without increased c-Myc occupancy during c-Myc induction (right). The differences in the levels of changes between H3K4Me3 and Cdk9 were significant (Welch's two-tailed t test) at core promoters (p value < 2.2×10^{-16}) and at enhancers with increased c-Myc occupancy (p value = 6.48×10^{-7}) and not significant at enhancers without increased c-Myc occupancy (p value = 0.06).

(B) Western blots of RNA Pol II at 0, 1, and 24 hr using antibodies specific to various forms of the enzyme. From top to bottom: RNA Pol II Ser2P specific (H5, Covance), RNA Pol II Ser2P specific (A300-654A, Bethyl), RNA Pol II Ser5P specific (H14, Covance), hypophosphorylated RNA Pol II specific (8WG16, Bethyl), total RNA Pol II (N-20, Santa Cruz). For RNA Pol II Ser2P and Ser5P antibodies, the ratio of signals versus 0 hr is displayed for each time point below the blot.

(C) Bar graph of mean ± SEM. RNA Pol II enrichment ratio between elongating and initiating regions during c-Myc induction at 0, 1, and 24 hr (left, center, and right) for the top 5,000 genes ranked by RNA Pol II occupancy at 0 hr. The *y* axis shows the ratio between the fold enrichment over background of RNA Pol II in the elongating region versus the fold enrichment over background of RNA Pol II in the promoter region. Changes between 0, 1, and 24 hr are significant (Welch's two-tailed t test, p value < 1×10^{-16}).

(D) Empirical cumulative distribution plots of RNA Pol II traveling ratios (TR) for 1,000 transcribed genes (Rahl et al., 2010). Genes were randomly selected from the pool of genes containing higher than background levels of RNA Pol II at the promoter and gene body at 0, 1, and 24 hr. Differences in the TR distribution at 0 and 24 hr are significant (Welch's two-tailed t test, p value = 4.5×10^{-5}).

(E) Left: Bar graph showing quantification of total RNA levels for cells at 0, 1, and 24 hr. Units are in ng of total RNA per 1,000 cells and represented as mean ± SEM. Right: 5% TBE urea gel of ethidium bromide stained total RNA extracted from equivalent numbers of cells at 0, 1, and 24 hr. Bands corresponding to the 5.8S rRNA subunit, 5S rRNA subunit, and tRNA are labeled.

(F) Boxplot of transcripts/cell estimations from NanoString nCounter gene expression assays for active (right) or silent (left) genes at 0, 1, and 24 hr; 755 active genes (expressed > 1 transcripts/cell) at 0 hr are shown (left, red). 514 silent genes (expressed < 0.5 transcripts/cell) at 0 hr are shown (right, black). The number of genes with increased expression between 0 and 1 hr are significant (Wilcoxon rank sum test) for active genes (p value < 2.2×10^{-16}) and nonsignificant for silent genes (p value = 0.997). See also Figure S3.

and 24 hr after induction (Figure 1). ChIP-Seq analysis revealed that c-Myc occupies both the core promoters and enhancers of actively transcribed genes in all three tumor types (Figures 4B–4D). Inspection of individual genes tracks showed c-Myc binding to the core promoters of individual genes and to active enhancers in the respective cell type (Figure 4E). For all three tumor types, the c-Myc binding sites at core promoters occurred at canonical E-box motifs, whereas c-Myc binding at enhancers occurred at variant E-box sequence motifs (Figure 4F). We conclude that in diverse tumor cells expressing elevated levels of c-Myc, the transcription factor consistently occupies sites at the promoters and enhancers of the majority of actively transcribed genes.

Effects of Differential c-Myc Expression in SCLC

MYC amplification in SCLC correlates with tumor progression and often occurs in association with recurrent disease (Johnson et al., 1987; Little et al., 1983). We used two different SCLC lines that express different levels of c-Myc to determine whether higher c-Myc levels are associated with increased promoter/enhancer occupancy and transcriptional amplification in patient-derived SCLC. H128 SCLC cells express relatively low levels of c-Myc from an unamplified *MYC* gene and H2171 SCLC cells express high levels of c-Myc due to amplification of a region on chromosome 8 with *MYC* (Campbell et al., 2008). Although these cells originate from different patients, they nonetheless provide a system to determine if the effects

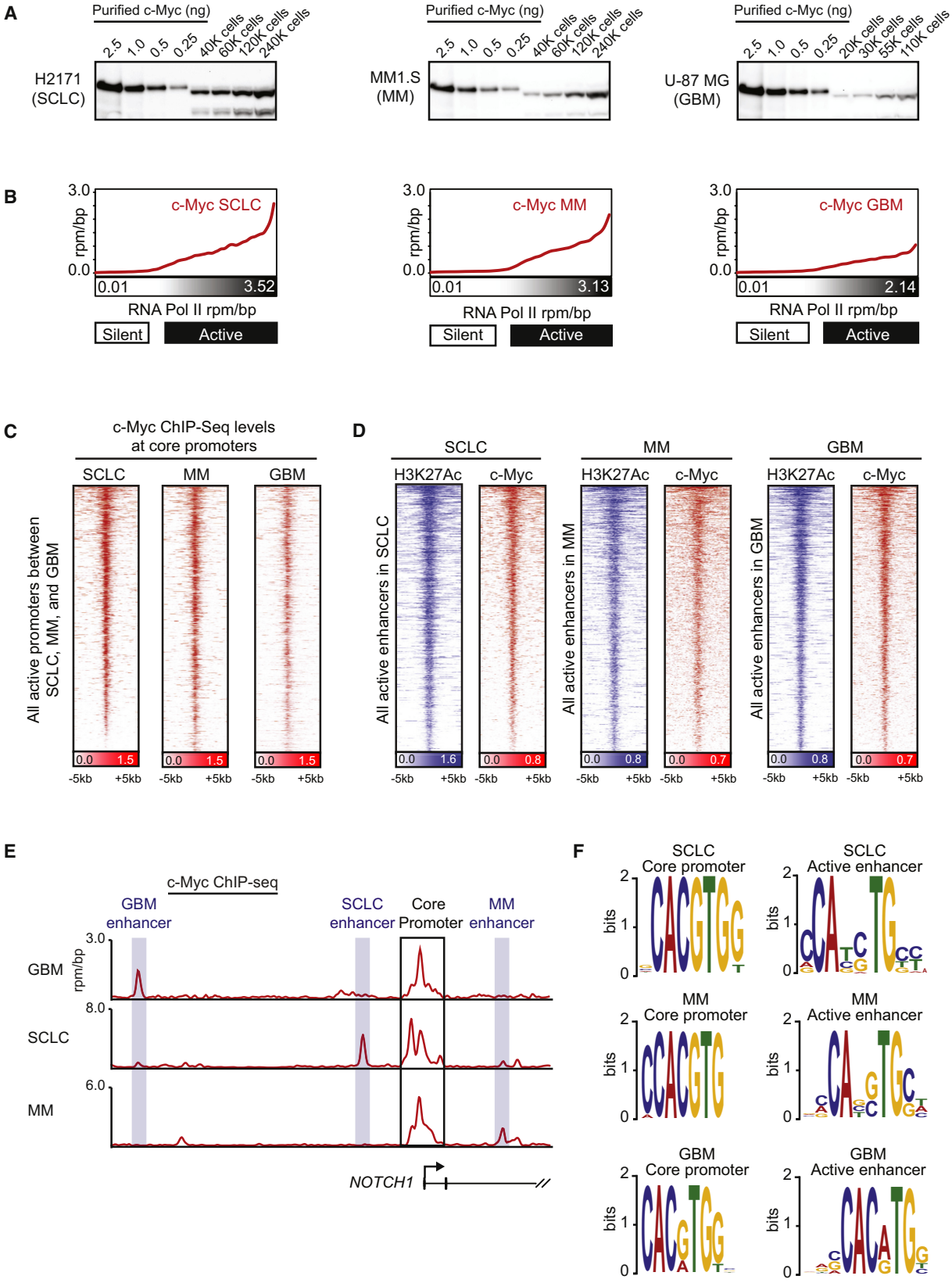
A
Purified c-Myc (ng)
2.5
1.0
0.5
0.25
40K cells
60K cells
120K cells
240K cells
H2171 (SCLC)
MM1.S (MM)
20K cells
30K cells
55K cells
110K cells
U-87 MG (GBM)
B
c-Myc SCLC
c-Myc MM
c-Myc GBM
rpm/bp
3.0
0.0
0.01
3.52
3.13
2.14
RNA Pol II rpm/bp
Silent
Active
C
c-Myc ChIP-Seq levels at core promoters
SCLC
MM
GBM
All active promoters between SCLC, MM, and GBM
0.0
1.5
-5kb
+5kb
D
H3K27Ac
c-Myc
All active enhancers in SCLC
All active enhancers in MM
All active enhancers in GBM
1.6
0.8
0.7
E
c-Myc ChIP-seq
GBM enhancer
SCLC enhancer
Core Promoter
MM enhancer
GBM
SCLC
MM
8.0
6.0
NOTCH1
F
SCLC Core promoter
SCLC Active enhancer
MM Core promoter
MM Active enhancer
GBM Core promoter
GBM Active enhancer
bits
2
1
0

of different levels of c-Myc observed in the Burkitt's lymphoma model are recapitulated by low and high endogenous expression in SCLC.

Analysis of the steady-state levels of c-Myc in these two SCLC cell lines revealed that there was approximately 150-fold more c-Myc protein in H2171 compared to H128 (Figure 5A; Figure S4A). c-Myc occupancy was associated with RNA Pol II occupancy genome-wide in both low and high c-Myc SCLC (Figure 5B). The set of transcribed genes was similar in low and high c-Myc SCLC, indicating that elevated c-Myc levels do not increase the number of expressed genes significantly (Figure S4B). SCLC cells with higher expression of c-Myc showed increased occupancy of core promoters and enhancers (Figure 5C) of active genes. Thus, the effects of increased levels of c-Myc on genome-wide occupancy that were observed in the Burkitt's lymphoma model were also observed in the SCLC tumor cells.

We then investigated whether SCLC cells with elevated c-Myc levels showed evidence of increased transcription elongation. SCLC cells expressing higher c-Myc levels (H2171) had a higher ratio of elongation-associated Ser2-phosphorylated RNA Pol II molecules (Figure 5D), and a small but significant increase in the levels of elongating RNA Pol II across the genome as measured by RNA Pol II ChIP-Seq enrichment (Figure 5E) and by RNA Pol II traveling ratio (Figure 5F). SCLC cells with elevated c-Myc levels showed increased levels of total RNA, tRNA, and rRNA (Figure 5G; Figure S4C). Digital gene expression (NanoString) analysis demonstrated that 88% of genes expressed at one transcript/cell or higher in low c-Myc cells were upregulated upon c-Myc induction, with an average 3.5-fold increase in expression (Figure 5H). In contrast, 93% of genes that were not expressed in cells with lower levels of c-Myc remained silent (Figure 5H). As with the inducible c-Myc system, these results indicate that the predominant effect of elevated levels of c-Myc in SCLC is transcriptional amplification of the existing gene expression program.

DISCUSSION

Elevated expression of c-Myc occurs frequently in human cancers and is associated with tumor aggression and a remarkable range of cellular phenotypes, but the effect of high levels of c-Myc on global gene regulation in tumor cells is poorly understood. A widely held view is that high levels of c-Myc lead to newly activated or repressed "Myc target genes." The results described here and by Nie et al. (2012) in this issue, support a different model: c-Myc accumulates in the promoter regions of active genes across the cancer cell genome and causes transcriptional amplification, producing increased levels of transcripts within the cell's gene expression program.

Transcription factors such as the myogenic regulator MyoD or the pluripotency regulators Oct4 and Sox2, when newly expressed at high levels in cells, will bind and establish new enhancers that modify the expression program and alter cell state (Graf and Enver, 2009). In contrast, expression of high levels of c-Myc in tumor cells produces a very different result. In the tumor cell systems described here, increased levels of c-Myc result in increased binding to active genes and little binding to genes that were inactive at low c-Myc levels, and there is little change in the set of actively transcribed genes. As the levels of c-Myc increase, high affinity E-box sites at active core promoters become saturated and lower affinity E-box variant sequences at promoters and enhancers become occupied. This behavior of c-Myc is consistent with evidence that the open chromatin environment at active promoters is important for binding by this factor (Guccione et al., 2006). Furthermore, enhancers loop into proximity of core promoters at active genes (Bulger and Groudine, 2011; Göndör and Ohlsson, 2009; Kagey et al., 2010; Ong and Corces, 2011) and this proximity may facilitate binding of c-Myc to nearby enhancer elements once binding to sites in core promoters is saturated. The functional consequence of elevated c-Myc binding at active genes is increased recruitment of the pause release factor P-TEFb, increased transcriptional elongation, and a global increase in transcript levels.

The model in which oncogenic c-Myc acts primarily in transcriptional amplification of the tumor cell's gene expression program provides an explanation for the diverse effects of oncogenic c-Myc on gene expression in different tumor cells. Numerous gene expression studies have identified sets of genes whose expression levels are altered by changes in c-Myc levels (Dang et al., 2006; Ji et al., 2011; Kim et al., 2006; Schlosser et al., 2005; Schuhmacher et al., 2001; Zeller et al., 2003). These c-Myc signatures vary greatly across cell types (Chandriani et al., 2009), making it difficult to ascribe the broad range of cellular effects produced by oncogenic c-Myc to a key set of target genes. This variation in c-Myc signatures would be expected with transcriptional amplification of the different gene expression

Figure 4. c-Myc Binds to Core Promoters and Active Enhancers when Overexpressed in Different Cancers

(A) Western blot of c-Myc protein levels in tumor cell lines compared with purified c-Myc. Increasing amounts of purified c-Myc (left lanes) and lysates prepared from increasing numbers of cells (right lanes) are shown for SCLC (left), MM (middle), and GBM (right).

(B) For each tumor cell line, median c-Myc levels in units of rpm/bp are plotted at promoters ranked by increasing RNA Pol II occupancy. Promoters were binned (50/bin) and a smoothing function was applied to median levels.

(C) For each tumor cell line, a heatmap of c-Myc levels at TSSs of actively transcribed genes is displayed. Each row represents the ±5 kb centered on the TSS. TSSs for actively transcribed genes in each tumor cell line are shown. Color scaled intensities are in units of rpm/bp.

(D) For each tumor cell line, a heatmap displays H3K27Ac and c-Myc levels at active enhancers. Each row represents the ±5 kb centered on the H3K27Ac peak. Rows are ordered by H3K27Ac binding in each tumor cell line. Color scaled intensities are in units of rpm/bp.

(E) c-Myc binding at the *NOTCH1* promoter in GBM (top), SCLC (middle), and MM (bottom) tumor cell lines. The *x* axis shows genomic position. The *y* axis shows signal of c-Myc occupancy (rpm/bp). The *NOTCH1* gene is indicated at the bottom (introns as lines, exons as boxes). Enhancer regions are shaded in light blue. The core promoter of *NOTCH1* is boxed in black.

(F) For each tumor cell line, the c-Myc binding motif found enriched at core promoters of actively transcribed genes and active enhancers is displayed (SCLC core promoter, $p < 4 \times 10^{-215}$; SCLC active enhancer, $p < 9 \times 10^{-1504}$; MM core promoter, $p < 6 \times 10^{-117}$; MM active enhancer, $p < 5 \times 10^{-678}$; GBM core promoter, $p < 1 \times 10^{-160}$; GBM active enhancer $p < 4 \times 10^{-635}$).

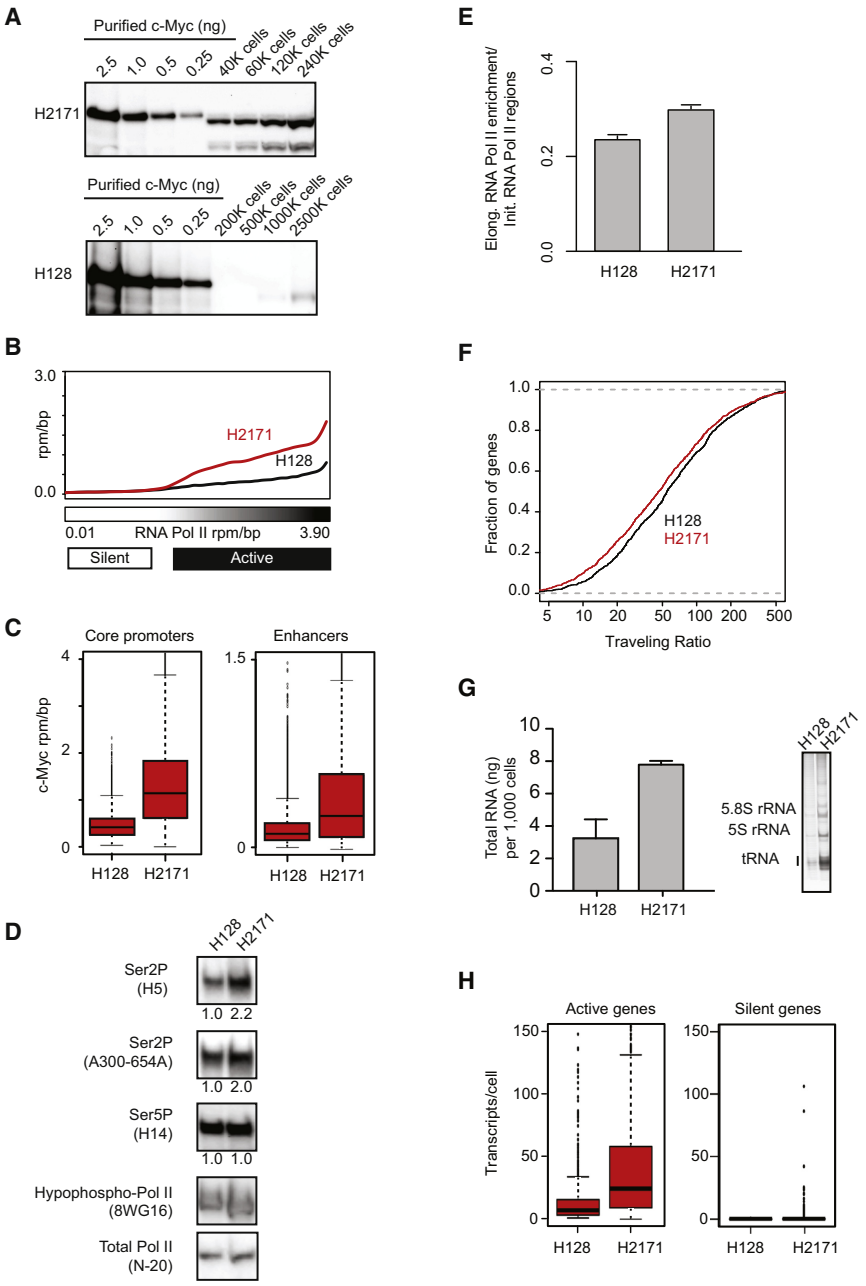

Figure 5. c-Myc Enhancer Invasion and Transcriptional Amplification in Patient-Derived Small Cell Lung Carcinoma

(A) c-Myc protein levels in small cell lung carcinoma for low c-Myc expressing (H128) and c-Myc overexpressing (H2171) tumor cells determined by quantitative Western Blot analysis with purified his_6-c-Myc.

(B) For low and high c-Myc SCLC, the median c-Myc levels in units of rpm/bp were plotted at promoters ranked by increasing RNA Pol II occupancy in H128. c-Myc levels are shown for H128 and H2171 SCLC (black, red). Promoters were binned (50/bin) and a smoothing function was applied to median levels.

(C) Left: Boxplots of c-Myc levels in the ±1 kb centered on TSSs at promoters of 15,000 actively transcribed genes in H128 and H2171. Right: Boxplot representation of c-Myc levels at 15,000 active enhancers in H128 and H2171. Units are in rpm/bp. Changes between mean c-Myc levels are significant (Welch's two-tailed t test) at promoters (p value < 2.2×10^{-16}) and enhancers (p value < 2.2×10^{-16}).

(D) Western blots of RNA Pol II in H128 and H2171 cells using antibodies specific to various forms of the enyzme. From top to bottom: RNA Pol II Ser2P specific (H5, Covance), RNA Pol II Ser2P specific (A300-654A, Bethyl), RNA Pol II Ser5P specific (H14, Covance), hypophosphorylated RNA Pol II specific (8WG16, Bethyl), total RNA Pol II (N-20, Santa Cruz). For RNA Pol II Ser2P and Ser5P antibodies, the ratio of signal versus H128 signal are displayed for each cell line below the blot.

(E) Bar graph of mean ± SEM. RNA Pol II enrichment ratio between elongating and initiating in H128 and H2171 cells for the top 5,000 genes ranked by RNA Pol II occupancy in H128 cells. The *y* axis shows the ratio between the fold enrichment over background of RNA Pol II in the elongating region versus the fold enrichment over background of RNA Pol II in the promoter region. Changes between H128 and H2171 cells are significant (Welch's two-tailed t test, p value < 1×10^{-16}).

(F) Empirical cumulative distribution plots of Pol II traveling ratios (TR) for 1,000 transcribed genes. Genes were randomly selected from the pool of genes containing higher than background levels of Pol II at the promoter and gene body in H128 and H2171 cells. Differences in the TR distribution between H128 and H2171 are significant (Welch's two-tailed t test, p value = 5×10^{-3}).

(G) Left: Bar graph showing quantification of total RNA levels for H128 and H2171 cells. Units are in ng of total RNA per 1,000 cells and represented as mean ± SEM. Right: 5% TBE urea gel of ethidium bromide stained total RNA extracted from equivalent numbers of cells from H128 and H2171. Bands corresponding to the 5.8S rRNA subunit, 5S rRNA subunit, and tRNA are labeled.

(H) Boxplots of transcripts/cell estimations from NanoString nCounter gene expression assays for active (right) or silent (left) genes in H128 and H2171 cells. 706 active genes (expressed > 1 transcripts/cell) in H128 cells are shown (left, red). 568 silent genes (exrpressed < 0.5 transcripts/cell) in H128 cells are shown (right, black). The number of genes with increased expression between H128 and H2171 cells are significant (Wilcoxon rank sum test) for active genes (p value < 2.2×10^{-16}) and nonsignificant for silent genes (p value = 0.03). See also Figure S4.

programs inherent in different cancer cells. Some variation in c-Myc signatures may also be due to a limitation of microarray-based analysis, which typically involves a normalization step that assumes similar levels of total RNA and thus does not detect amplification of the entire gene expression program. Although our evidence indicates that c-Myc functions primarily in amplification, there are a small number of genes whose expression is reduced in cells with high levels of c-Myc. These

genes may be directly repressed by c-Myc or their repression may be due to indirect effects; for example, elevated levels of a negative regulator might overwhelm c-Myc-induced amplification of some genes.

Transcriptional amplification may explain why c-Myc plays a critical role in tumorigenesis in a wide variety of human tissues. Although numerous cellular pathways can be mutated to provide an initial signal for increased cell growth and proliferation, transcriptional amplification could provide the sweeping changes in cellular physiology necessary for aggressive cellular growth and proliferation. Translational capacity and aerobic energy metabolism are among the cellular functions that are limiting for the growth of tumor cells and an increase in the levels of transcripts for this machinery would increase the levels of its rate limiting components (Dai and Lu, 2008; Ruggero, 2009). It is also possible that the increase in essentially all components of the gene expression program provides cells with an advantage when adapting to the multiple mutated pathways that characterize most tumor cells.

Elevated expression of c-Myc occurs frequently in cancer. The model that c-Myc can promote tumorigenesis through transcriptional amplification suggests that therapies focused on the molecular mechanisms involved in RNA Pol II pause control and elongation may be valuable for clinical treatment of many different tumors.

EXPERIMENTAL PROCEDURES

Cell Culture

Small-cell lung carcinoma cells H128 (HTB-120 ATCC) and H2171 (CRL-5929) were kindly provided by John Minna, UT Southwestern and P493-6 cells were kindly provided by Chi Van Dang, University of Pennsylvania. Multiple myeloma cells MM1.S (CRL-2974 ATCC) and U-87 MG cells (HTB-14 ATCC) were purchased from ATCC. Unless otherwise stated, all cells were propagated in RPMI-1640 supplemented with 10% fetal bovine serum and 1% GlutaMAX (Invitrogen, 35050-061). U-87 MG cells were cultured in Eagle's Minimum Essential Medium (EMEM) modified to contain Earles Balanced Salt Solution, nonessential amino acids, 2 mM L-glutamine, 1 mM sodium pyruvate, and 1,500 mg/l sodium bicarbonate. Cells were grown at 37°C and 5% CO_2.

For c-Myc induction experiments, the conditional p*myc*-tet construct in P493-6 cells was repressed with 0.1 μg/ml tetracycline (Sigma, T7660) for 72 hr. *MYC* expression was induced by three washes with RPMI-1640 medium containing 10% tetracycline system approved FBS (Clontech, 631105) and 1% GlutaMAX.

Quantitative Western Blotting

Quantitative western blotting was carried out as previously described (Rudolph et al., 1999). For every protein preparation (total protein extraction), cell number was determined by counting cells with C-Chip disposable hemocytometers (Digital Bio). Cells were lysed at a concentration of 100,000 cells/μl lysis buffer and processed as described above. Purified, recombinant full-length his_6-c-Myc was used as a standard and loaded at the concentrations depicted in each figure. Determination of the number of c-Myc protein molecules per cell was carried out by linear regression analysis using the Image Lab Software (Bio-Rad, version 3.0).

Protein Purification

Purified his_6-c-Myc and his_6-Max was generated in BL21(DE3) RIL *E. coli* essentially the same as described in (Farina et al., 2004) except c-Myc and Max were purified individually. Constructs were kindly provided by Ernest Martinez (UC Riverside) and his_6-c-Myc was subcloned into pET15b prior to purification. Purified protein was stored as glycerol stocks (40% glycerol, 50 mM Tris [pH 8.0], 150 mM NaCl) at −80°C.

c-Myc/Max Gelshift Experiments

Purified recombinant his_6-c-Myc and his_6-Max were used to test the ability of c-Myc/Max heterodimers to bind E-box variants in vitro using similar conditions described in (Ecevit et al., 2010). In brief, biotinylated Ebox DNA was competed with the indicated amounts of nonbiotinylated Ebox variant.

Chromatin Immunoprecipitation

ChIP was carried out as described in Rahl et al. (2010). Antibodies used are as follows: Total Pol II (Rpb1 N-terminus), Santa Cruz sc-899 lot# B1010; c-Myc (N-262), Santa Cruz sc-764 lot#G0111; Max (C-17), Santa Cruz sc-197 lot#A0311; Histone H3K27Ac, Abcam ab4729 lot#GR45787-1; Med1, Bethyl Labs A300-793A lot#A300-793A-1; Histone H3K4me3, Millipore 07-473 lot#-DAM1824767; and Cdk9, Santa Cruz sc-8338 lot# I0109 and Santa Cruz sc-484 lot# B0910.

Illumina Sequencing and Library Generation

Purified ChIP DNA was used to prepare Illumina multiplexed sequencing libraries. Libraries for Illumina sequencing were prepared following the Illumina TruSeq DNA Sample Preparation v2 kit protocol with the selected exceptions described in supplemental methods.

Data Analysis

All ChIP-Seq data sets were aligned using Bowtie (version 0.12.2) (Langmead et al., 2009) to build version NCBI36/HG18 of the human genome. Aligned and raw data can be found online associated with the GEO Accession ID GSE36354.

We used a simple method to calculate the normalized read density of a ChIP-Seq data set in any region. ChIP-Seq reads aligning to the region were extended by 200 bp and the density of reads per base pair (bp) was calculated. The density of reads in each region was normalized to the total number of million mapped reads producing read density in units of reads per million mapped reads per bp (rpm/bp).

We used the MACS version 1.4.1 (Model based analysis of ChIP-Seq) (Zhang et al., 2008) peak finding algorithm to identify regions of ChIP-Seq enrichment over background. A p value threshold of enrichment of 1×10^{-9} was used for all data sets. In order to display c-Myc binding at promoters, we first calculated the c-Myc ChIP-Seq density (rpm/bp) in 50 bp bins ± 5 kb around the transcription start site (TSS) of transcribed genes. Promoters were ranked by average c-Myc density and the c-Myc density in each bin was shaded based on intensity. In order to quantify changes in c-Myc occupancy at promoters, the mean ChIP-Seq density in units of rpm/bp was calculated for the ±1 kb region around the TSS of transcribed genes. The distribution of mean ChIP-Seq densities was compared between samples using a Welch's two-tailed t test. A similar approach was used to quantify c-Myc binding at enhancers, where instead of centering regions on the TSS, the center of the enriched region for H3K27Ac was used. Active enhancers were defined as regions of enrichment for H3K27Ac outside of promoters (greater than 5 kb away from any TSS).

SUPPLEMENTAL INFORMATION

Supplemental Information includes Extended Experimental Procedures, four figures, and five tables and can be found with this article online at http://dx.doi.org/10.1016/j.cell.2012.08.026.

ACKNOWLEDGMENTS

We thank John Minna and Chi Dang for cell lines; Ernest Martinez for constructs; David Orlando for bioinformatics support; Tom Volkert, Jennifer Love, Sumeet Gupta, and Vidya Dhanapal at the Whitehead Genome Technologies Core for Solexa sequencing; Nancy Hannett for cloning support; Jessica Reddy for assistance with FACS; Darin Fogg, Amins Corporation, and Nathan Elliott, NanoString, for excellent technical support; and Michael Cole and members of the Young, Burge and Bradner labs for helpful discussion. This work was supported by National Institutes of Health grants HG002668 (R.A.Y.) and CA146445 (R.A.Y., T.I.L.), Swedish Research Council Postdoctoral Fellowship

VR-B0086301 (J.L.), American Cancer Society Postdoctoral Fellowship PF-11-042- 01-DMC (P.B.R.) and Damon-Runyon Cancer Research Foundation (J.E.B). J.E.B. and R.A.Y. are founders of Syros Pharmaceuticals.

Received: March 8, 2012
Revised: May 29, 2012
Accepted: August 8, 2012
Published: September 27, 2012

REFERENCES

Amati, B., Alevizopoulos, K., and Vlach, J. (1998). Myc and the cell cycle. Front. Biosci. *3*, d250–d268.

Amati, B., Frank, S.R., Donjerkovic, D., and Taubert, S. (2001). Function of the c-Myc oncoprotein in chromatin remodeling and transcription. Biochim. Biophys. Acta *1471*, M135–M145.

Arabi, A., Wu, S., Ridderstråle, K., Bierhoff, H., Shiue, C., Fatyol, K., Fahlén, S., Hydbring, P., Söderberg, O., Grummt, I., et al. (2005). c-Myc associates with ribosomal DNA and activates RNA polymerase I transcription. Nat. Cell Biol. *7*, 303–310.

Beroukhim, R., Mermel, C.H., Porter, D., Wei, G., Raychaudhuri, S., Donovan, J., Barretina, J., Boehm, J.S., Dobson, J., Urashima, M., et al. (2010). The landscape of somatic copy-number alteration across human cancers. Nature *463*, 899–905.

Blackwood, E.M., and Eisenman, R.N. (1991). Max: a helix-loop-helix zipper protein that forms a sequence-specific DNA-binding complex with Myc. Science *251*, 1211–1217.

Blackwood, E.M., Lüscher, B., and Eisenman, R.N. (1992). Myc and Max associate in vivo. Genes Dev. *6*, 71–80.

Bouchard, C., Marquardt, J., Brás, A., Medema, R.H., and Eilers, M. (2004). Myc-induced proliferation and transformation require Akt-mediated phosphorylation of FoxO proteins. EMBO J. *23*, 2830–2840.

Brès, V., Yoshida, T., Pickle, L., and Jones, K.A. (2009). SKIP interacts with c-Myc and Menin to promote HIV-1 Tat transactivation. Mol. Cell *36*, 75–87.

Bulger, M., and Groudine, M. (2011). Functional and mechanistic diversity of distal transcription enhancers. Cell *144*, 327–339.

Campbell, P.J., Stephens, P.J., Pleasance, E.D., O'Meara, S., Li, H., Santarius, T., Stebbings, L.A., Leroy, C., Edkins, S., Hardy, C., et al. (2008). Identification of somatically acquired rearrangements in cancer using genome-wide massively parallel paired-end sequencing. Nat. Genet. *40*, 722–729.

Chandriani, S., Frengen, E., Cowling, V.H., Pendergrass, S.A., Perou, C.M., Whitfield, M.L., and Cole, M.D. (2009). A core MYC gene expression signature is prominent in basal-like breast cancer but only partially overlaps the core serum response. PLoS ONE *4*, e6693.

Chen, X., Xu, H., Yuan, P., Fang, F., Huss, M., Vega, V.B., Wong, E., Orlov, Y.L., Zhang, W., Jiang, J., et al. (2008). Integration of external signaling pathways with the core transcriptional network in embryonic stem cells. Cell *133*, 1106–1117.

Cole, M.D., and Cowling, V.H. (2008). Transcription-independent functions of MYC: regulation of translation and DNA replication. Nat. Rev. Mol. Cell Biol. *9*, 810–815.

Cowling, V.H., and Cole, M.D. (2010). Myc Regulation of mRNA Cap Methylation. Genes Cancer *1*, 576–579.

Dai, M.S., and Lu, H. (2008). Crosstalk between c-Myc and ribosome in ribosomal biogenesis and cancer. J. Cell. Biochem. *105*, 670–677.

Dang, C.V. (2010). Rethinking the Warburg effect with Myc micromanaging glutamine metabolism. Cancer Res. *70*, 859–862.

Dang, C.V. (2012). MYC on the path to cancer. Cell *149*, 22–35.

Dang, C.V., O'Donnell, K.A., Zeller, K.I., Nguyen, T., Osthus, R.C., and Li, F. (2006). The c-Myc target gene network. Semin. Cancer Biol. *16*, 253–264.

Eberhardy, S.R., and Farnham, P.J. (2001). c-Myc mediates activation of the cad promoter via a post-RNA polymerase II recruitment mechanism. J. Biol. Chem. *276*, 48562–48571.

Eberhardy, S.R., and Farnham, P.J. (2002). Myc recruits P-TEFb to mediate the final step in the transcriptional activation of the cad promoter. J. Biol. Chem. *277*, 40156–40162.

Ecevit, O., Khan, M.A., and Goss, D.J. (2010). Kinetic analysis of the interaction of b/HLH/Z transcription factors Myc, Max, and Mad with cognate DNA. Biochemistry *49*, 2627–2635.

Eilers, M., and Eisenman, R.N. (2008). Myc's broad reach. Genes Dev. *22*, 2755–2766.

Facchini, L.M., and Penn, L.Z. (1998). The molecular role of Myc in growth and transformation: recent discoveries lead to new insights. FASEB J. *12*, 633–651.

Farina, A., Faiola, F., and Martinez, E. (2004). Reconstitution of an E box-binding Myc:Max complex with recombinant full-length proteins expressed in Escherichia coli. Protein Expr. Purif. *34*, 215–222.

Felsher, D.W., and Bishop, J.M. (1999). Reversible tumorigenesis by MYC in hematopoietic lineages. Mol. Cell *4*, 199–207.

Fernandez, P.C., Frank, S.R., Wang, L., Schroeder, M., Liu, S., Greene, J., Cocito, A., and Amati, B. (2003). Genomic targets of the human c-Myc protein. Genes Dev. *17*, 1115–1129.

Flores, I., Murphy, D.J., Swigart, L.B., Knies, U., and Evan, G.I. (2004). Defining the temporal requirements for Myc in the progression and maintenance of skin neoplasia. Oncogene *23*, 5923–5930.

Gallant, P. (2005). Myc, cell competition, and compensatory proliferation. Cancer Res. *65*, 6485–6487.

Gargano, B., Amente, S., Majello, B., and Lania, L. (2007). P-TEFb is a crucial co-factor for Myc transactivation. Cell Cycle *6*, 2031–2037.

Geiss, G.K., Bumgarner, R.E., Birditt, B., Dahl, T., Dowidar, N., Dunaway, D.L., Fell, H.P., Ferree, S., George, R.D., Grogan, T., et al. (2008). Direct multiplexed measurement of gene expression with color-coded probe pairs. Nat. Biotechnol. *26*, 317–325.

Gomez-Roman, N., Grandori, C., Eisenman, R.N., and White, R.J. (2003). Direct activation of RNA polymerase III transcription by c-Myc. Nature *421*, 290–294.

Göndör, A., and Ohlsson, R. (2009). Chromosome crosstalk in three dimensions. Nature *461*, 212–217.

Graf, T., and Enver, T. (2009). Forcing cells to change lineages. Nature *462*, 587–594.

Grandori, C., Gomez-Roman, N., Felton-Edkins, Z.A., Ngouenet, C., Galloway, D.A., Eisenman, R.N., and White, R.J. (2005). c-Myc binds to human ribosomal DNA and stimulates transcription of rRNA genes by RNA polymerase I. Nat. Cell Biol. *7*, 311–318.

Guccione, E., Martinato, F., Finocchiaro, G., Luzi, L., Tizzoni, L., Dall' Olio, V., Zardo, G., Nervi, C., Bernard, L., and Amati, B. (2006). Myc-binding-site recognition in the human genome is determined by chromatin context. Nat. Cell Biol. *8*, 764–770.

Hanahan, D., and Weinberg, R.A. (2011). Hallmarks of cancer: the next generation. Cell *144*, 646–674.

Herold, S., Herkert, B., and Eilers, M. (2009). Facilitating replication under stress: an oncogenic function of MYC? Nat. Rev. Cancer *9*, 441–444.

Hirvonen, H.E., Salonen, R., Sandberg, M.M., Vuorio, E., Västrik, I., Kotilainen, E., and Kalimo, H. (1994). Differential expression of myc, max and RB1 genes in human gliomas and glioma cell lines. Br. J. Cancer *69*, 16–25.

Hoffman, B., and Liebermann, D.A. (2008). Apoptotic signaling by c-MYC. Oncogene *27*, 6462–6472.

Hurlin, P.J., and Dezfouli, S. (2004). Functions of myc:max in the control of cell proliferation and tumorigenesis. Int. Rev. Cytol. *238*, 183–226.

Jain, M., Arvanitis, C., Chu, K., Dewey, W., Leonhardt, E., Trinh, M., Sundberg, C.D., Bishop, J.M., and Felsher, D.W. (2002). Sustained loss of a neoplastic phenotype by brief inactivation of MYC. Science *297*, 102–104.

Ji, H., Wu, G., Zhan, X., Nolan, A., Koh, C., De Marzo, A., Doan, H.M., Fan, J., Cheadle, C., Fallahi, M., et al. (2011). Cell-type independent MYC target genes reveal a primordial signature involved in biomass accumulation. PLoS ONE *6*, e26057.

Johnson, B.E., Ihde, D.C., Makuch, R.W., Gazdar, A.F., Carney, D.N., Oie, H., Russell, E., Nau, M.M., and Minna, J.D. (1987). myc family oncogene amplification in tumor cell lines established from small cell lung cancer patients and its relationship to clinical status and course. J. Clin. Invest. *79*, 1629–1634.

Kagey, M.H., Newman, J.J., Bilodeau, S., Zhan, Y., Orlando, D.A., van Berkum, N.L., Ebmeier, C.C., Goossens, J., Rahl, P.B., Levine, S.S., et al. (2010). Mediator and cohesin connect gene expression and chromatin architecture. Nature *467*, 430–435.

Kanazawa, S., Soucek, L., Evan, G., Okamoto, T., and Peterlin, B.M. (2003). c-Myc recruits P-TEFb for transcription, cellular proliferation and apoptosis. Oncogene *22*, 5707–5711.

Kidder, B.L., Yang, J., and Palmer, S. (2008). Stat3 and c-Myc genome-wide promoter occupancy in embryonic stem cells. PLoS ONE *3*, e3932.

Kim, Y.H., Girard, L., Giacomini, C.P., Wang, P., Hernandez-Boussard, T., Tibshirani, R., Minna, J.D., and Pollack, J.R. (2006). Combined microarray analysis of small cell lung cancer reveals altered apoptotic balance and distinct expression signatures of MYC family gene amplification. Oncogene *25*, 130–138.

Kuttler, F., and Mai, S. (2006). c-Myc, Genomic Instability and Disease. Genome Dyn. *1*, 171–190.

Langmead, B., Trapnell, C., Pop, M., and Salzberg, S.L. (2009). Ultrafast and memory-efficient alignment of short DNA sequences to the human genome. Genome Biol. *10*, R25.

Li, Z., Van Calcar, S., Qu, C., Cavenee, W.K., Zhang, M.Q., and Ren, B. (2003). A global transcriptional regulatory role for c-Myc in Burkitt's lymphoma cells. Proc. Natl. Acad. Sci. USA *100*, 8164–8169.

Lin, C.J., Malina, A., and Pelletier, J. (2009). c-Myc and eIF4F constitute a feedforward loop that regulates cell growth: implications for anticancer therapy. Cancer Res. *69*, 7491–7494.

Little, C.D., Nau, M.M., Carney, D.N., Gazdar, A.F., and Minna, J.D. (1983). Amplification and expression of the c-myc oncogene in human lung cancer cell lines. Nature *306*, 194–196.

Meyer, N., and Penn, L.Z. (2008). Reflecting on 25 years with MYC. Nat. Rev. Cancer *8*, 976–990.

Nesbit, C.E., Tersak, J.M., and Prochownik, E.V. (1999). MYC oncogenes and human neoplastic disease. Oncogene *18*, 3004–3016.

Nie, Z., Hu, G., Wei, G., Cui, K., Yamane, A., Resch, W., Wang, R., Green, D.R., Tessarollo, L., Casellas, R., et al. (2012). c-Myc Is a Universal Amplifier of Expressed Genes in Lymphocytes and Embryonic Stem Cells. Cell *151*, this issue, 68–79.

Nieminen, A.I., Partanen, J.I., and Klefstrom, J. (2007). c-Myc blazing a trail of death: coupling of the mitochondrial and death receptor apoptosis pathways by c-Myc. Cell Cycle *6*, 2464–2472.

Nilsson, J.A., and Cleveland, J.L. (2003). Myc pathways provoking cell suicide and cancer. Oncogene *22*, 9007–9021.

Ong, C.T., and Corces, V.G. (2011). Enhancer function: new insights into the regulation of tissue-specific gene expression. Nat. Rev. Genet. *12*, 283–293.

Pajic, A., Spitkovsky, D., Christoph, B., Kempkes, B., Schuhmacher, M., Staege, M.S., Brielmeier, M., Ellwart, J., Kohlhuber, F., Bornkamm, G.W., et al. (2000). Cell cycle activation by c-myc in a burkitt lymphoma model cell line. Int. J. Cancer *87*, 787–793.

Pelengaris, S., Littlewood, T., Khan, M., Elia, G., and Evan, G. (1999). Reversible activation of c-Myc in skin: induction of a complex neoplastic phenotype by a single oncogenic lesion. Mol. Cell *3*, 565–577.

Peterson, C.W., and Ayer, D.E. (2011). An extended Myc network contributes to glucose homeostasis in cancer and diabetes. Front. Biosci. *16*, 2206–2223.

Pomerantz, M.M., Ahmadiyeh, N., Jia, L., Herman, P., Verzi, M.P., Doddapaneni, H., Beckwith, C.A., Chan, J.A., Hills, A., Davis, M., et al. (2009). The 8q24 cancer risk variant rs6983267 shows long-range interaction with MYC in colorectal cancer. Nat. Genet. *41*, 882–884.

Prendergast, G.C., Lawe, D., and Ziff, E.B. (1991). Association of Myn, the murine homolog of max, with c-Myc stimulates methylation-sensitive DNA binding and ras cotransformation. Cell *65*, 395–407.

Prochownik, E.V. (2008). c-Myc: linking transformation and genomic instability. Curr. Mol. Med. *8*, 446–458.

Rahl, P.B., Lin, C.Y., Seila, A.C., Flynn, R.A., McCuine, S., Burge, C.B., Sharp, P.A., and Young, R.A. (2010). c-Myc regulates transcriptional pause release. Cell *141*, 432–445.

Rudolph, C., Adam, G., and Simm, A. (1999). Determination of copy number of c-Myc protein per cell by quantitative Western blotting. Anal. Biochem. *269*, 66–71.

Ruggero, D. (2009). The role of Myc-induced protein synthesis in cancer. Cancer Res. *69*, 8839–8843.

Schlosser, I., Hölzel, M., Hoffmann, R., Burtscher, H., Kohlhuber, F., Schuhmacher, M., Chapman, R., Weidle, U.H., and Eick, D. (2005). Dissection of transcriptional programmes in response to serum and c-Myc in a human B-cell line. Oncogene *24*, 520–524.

Schuhmacher, M., Staege, M.S., Pajic, A., Polack, A., Weidle, U.H., Bornkamm, G.W., Eick, D., and Kohlhuber, F. (1999). Control of cell growth by c-Myc in the absence of cell division. Curr. Biol. *9*, 1255–1258.

Schuhmacher, M., Kohlhuber, F., Hölzel, M., Kaiser, C., Burtscher, H., Jarsch, M., Bornkamm, G.W., Laux, G., Polack, A., Weidle, U.H., and Eick, D. (2001). The transcriptional program of a human B cell line in response to Myc. Nucleic Acids Res. *29*, 397–406.

Secombe, J., Pierce, S.B., and Eisenman, R.N. (2004). Myc: a weapon of mass destruction. Cell *117*, 153–156.

Shchors, K., and Evan, G. (2007). Tumor angiogenesis: cause or consequence of cancer? Cancer Res. *67*, 7059–7061.

Shou, Y., Martelli, M.L., Gabrea, A., Qi, Y., Brents, L.A., Roschke, A., Dewald, G., Kirsch, I.R., Bergsagel, P.L., and Kuehl, W.M. (2000). Diverse karyotypic abnormalities of the c-myc locus associated with c-myc dysregulation and tumor progression in multiple myeloma. Proc. Natl. Acad. Sci. USA *97*, 228–233.

Singh, A.M., and Dalton, S. (2009). The cell cycle and Myc intersect with mechanisms that regulate pluripotency and reprogramming. Cell Stem Cell *5*, 141–149.

Sodir, N.M., Swigart, L.B., Karnezis, A.N., Hanahan, D., Evan, G.I., and Soucek, L. (2011). Endogenous Myc maintains the tumor microenvironment. Genes Dev. *25*, 907–916.

Soucek, L., Whitfield, J., Martins, C.P., Finch, A.J., Murphy, D.J., Sodir, N.M., Karnezis, A.N., Swigart, L.B., Nasi, S., and Evan, G.I. (2008). Modelling Myc inhibition as a cancer therapy. Nature *455*, 679–683.

van Riggelen, J., Yetil, A., and Felsher, D.W. (2010). MYC as a regulator of ribosome biogenesis and protein synthesis. Nat. Rev. Cancer *10*, 301–309.

Verbeek, S., van Lohuizen, M., van der Valk, M., Domen, J., Kraal, G., and Berns, A. (1991). Mice bearing the E mu-myc and E mu-pim-1 transgenes develop pre-B-cell leukemia prenatally. Mol. Cell. Biol. *11*, 1176–1179.

Wright, J.B., Brown, S.J., and Cole, M.D. (2010). Upregulation of c-MYC in cis through a large chromatin loop linked to a cancer risk-associated single-nucleotide polymorphism in colorectal cancer cells. Mol. Cell. Biol. *30*, 1411–1420.

Zeller, K.I., Jegga, A.G., Aronow, B.J., O'Donnell, K.A., and Dang, C.V. (2003). An integrated database of genes responsive to the Myc oncogenic transcription factor: identification of direct genomic targets. Genome Biol. *4*, R69.

Zeller, K.I., Zhao, X., Lee, C.W., Chiu, K.P., Yao, F., Yustein, J.T., Ooi, H.S., Orlov, Y.L., Shahab, A., Yong, H.C., et al. (2006). Global mapping of c-Myc binding sites and target gene networks in human B cells. Proc. Natl. Acad. Sci. USA *103*, 17834–17839.

Zhang, Y., Liu, T., Meyer, C.A., Eeckhoute, J., Johnson, D.S., Bernstein, B.E., Nusbaum, C., Myers, R.M., Brown, M., Li, W., and Liu, X.S. (2008). Model-based analysis of ChIP-Seq (MACS). Genome Biol. *9*, R137.

Zhou, Q., Li, T., and Price, D.H. (2012). RNA polymerase II elongation control. Annu. Rev. Biochem. *81*, 119–143.